Pharmaceutical Nanotechnology

In vivo evaluation of safety of nanoporous silicon carriers following single and multiple dose intravenous administrations in mice

T. Tanaka [a,1], B. Godin [e,*,1], R. Bhavane [a], R. Nieves-Alicea [a], J. Gu [a], X. Liu [e], C. Chiappini [e], J.R. Fakhoury [e], S. Amra [e], A. Ewing [a], Q. Li [e], I.J. Fidler [b], M. Ferrari [c,d,e,*]

[a] Department of NanoMedicine and Biomedical Engineering, University of Texas Health Science Center, 1825 Pressler, Suite 537, Houston, TX 77030, USA
[b] Cancer Metastasis Research Center, Unit 854, University of Texas MD Anderson Cancer Center, 1515 Holcombe Blvd., Houston, TX 77030, USA
[c] Department of Experimental Therapeutics, Unit 422, University of Texas MD Anderson Cancer Center, 1515 Holcombe Blvd., Houston, TX 77030, USA
[d] Department of Bioengineering, Rice University, Houston, TX 77005, USA
[e] The Methodist Hospital Research Institute, 6670 Bertner St., Houston, TX 77030, USA

A B S T R A C T

Porous silicon (pSi) is being extensively studied as an emerging material for use in biomedical applications, including drug delivery, based on the biodegradability and versatile chemical and biophysical properties. We have recently introduced multistage nanoporous silicon microparticles (S1MP) designed as a cargo for nanocarrier drug delivery to enable the loaded therapeutics and diagnostics to sequentially overcome the biological barriers in order to reach their target. In this first report on biocompatibility of intravenously administered pSi structures, we examined the tolerability of negatively (-32.5 ± 3.1 mV) and positively (8.7 ± 2.5 mV) charged S1MP in acute single dose (10^7, 10^8, 5×10^8 S1MP/animal) and subchronic multiple dose (10^8 S1MP/animal/week for 4 weeks) administration schedules. Our data demonstrate that S1MP did not change plasma levels of renal (BUN and creatinine) and hepatic (LDH) biomarkers as well as 23 plasma cytokines. LDH plasma levels of 145.2 ± 23.6, 115.4 ± 29.1 vs. 127.0 ± 10.4; and 155.8 ± 38.4, 135.5 ± 52.3 vs. 178.4 ± 74.6 were detected in mice treated with 10^8 negatively charged S1MP, 10^8 positively charged S1MP vs. saline control in single and multiple dose schedules, respectively. The S1MPs did not alter LDH levels in liver and spleen, nor lead to infiltration of leukocytes into the liver, spleen, kidney, lung, brain, heart, and thyroid. Collectively, these data provide evidence of a safe intravenous administration of S1MPs as a drug delivery carrier.

© 2010 Elsevier B.V. All rights reserved.

1. Introduction

Porous silicon (pSi) based nanostructured materials are widely studied for use in biomedical applications based on their biodegradability in the physiological environment as well as readily modified physico-chemical and biophysical properties, including surface functionalization, size, shape and porosity (Anglin et al., 2008; Cerami, 1992; Salonen et al., 2005, 2008). Various pSi based platforms are under development for applications such as biomolecular screening (Nijdam et al., 2007, 2009), optical biosensing (Lehmann and Gosele, 1991; Lin et al., 1997), drug delivery through injectable carriers (Li et al., 2003; Tasciotti et al., 2008), implantable devices (Sharma et al., 2006), and orally administered medications with improved bioavailability (Salonen et al., 2005). For drug delivery application, biocompatibility presents one of the most important requirements. The first report on the biocompatibility of pSi structures in mid 1990s (Canham, 1995) described that the porosification of the silicon imparted biodegradation properties to the material. The degradation product of pSi structures is orthosilicic acid, composed of $Si(OH)_4$ units. Porous Si structures allow for the release of harmless silicic acid in aqueous solutions in the physiological pH range through hydrolysis of the Si–O bonds, (Jugdaohsingh et al., 2002) which is subsequently excreted in the urine through the kidneys (Carlisle, 1970). While the physiologic function of silicic acid is not clearly understood, the significant role of orthisilicic acid in bone and collagen growth was reported (Martin, 2007).

We have recently proposed multistage delivery system, in which the pSi particles, or so called 1st stage particles (S1MP) with the dimensions of several hundred of nm to a few microns, accommodate 2nd stage therapeutic nanoparticles (S2NP) (up to 100 nm in size) in their porous structure (Tasciotti et al., 2008). The idea behind the design of this delivery system is to enable the loaded therapeutic nanoparticles to sequentially overcome biological barriers and reach their target (Riehemann et al., 2009; Sakamoto et al., 2007; Tanaka et al., 2010; Tasciotti et al., 2008). This approach takes

into consideration that no single agent can be multi-tasking enough to bear functions enabling to overcome barriers of various origins. These carriers (Ferrari, 2010), are therapeutic multi-component constructs specifically engineered to avoid biological barriers, in which the functions of biological recognition, cytotoxicity and biological barrier avoidance are decoupled, yet act in efficacious operational harmony. Among the important bio-barriers for efficient delivery of therapeutic agents to tumors are hemorheology, efficient adhesion to the site of action, endothelial barrier and intracellular delivery. Based on the rational design guided by a mathematical toolset and in order to obtain the desired functionality, the effect of geometry on the vascular navigation behavior of micro and nanoparticles was studied. On the basis of the rational design, hemispherical shape was found to be beneficial upon the spherical one for margination towards vasculature wall in the circulation, biodistribution, endothelial adhesion, and cell internalization (Decuzzi et al., 2004; Lee et al., 2009; Ruoslahti, 2004). The ability of S1MP to overcome biological barriers such as cellular membrane, hemorheology, reticulo-endothelial system uptake was confirmed in a number of studies (Godin et al., 2010; Lee et al., 2009; Serda et al., 2009b,c).

The system is versatile and the size, shape, porosity, and pore size of S1MP can be finely tuned during the manufacturing processes (Canham, 1999; Cohen et al., 2003; Serda et al., 2009a). Moreover, physico-chemical properties of these particles can be tailored through their surface modifications, producing vectors with various surface characteristics and charges.

In this study, we examined the effect of S1MP following single- and multiple intravenous administrations in immunocompetent mice on the plasma levels for biomarkers of hepatic, muscular and renal injury, as well as levels of multiple cytokines and histological evaluation of major organs.

2. Methods

2.1. Fabrication, surface modification and characterization of porous silicon particles

Nanoporous quasi-hemispherical S1MPs were designed and fabricated in the Microelectronics Research Center at The University of Texas at Austin. The mean particle diameter was $1.6 \pm 0.2\,\mu m$, with pore size of $36.3 \pm 13.4\,nm$. Briefly, heavily doped p++ type (1 0 0) silicon wafers with resistivity of $0.005\,\Omega$-cm (Silicon Quest, Inc., Santa Clara, CA) were used as the silicon source. Silicon nitride (Si_3N_4) was deposited on the wafer by Low Pressure Chemical Vapor Deposition and standard photolithography was used to pattern the microparticles over the wafer using a contact aligner (K. Suss MA6 mask aligner) and AZ5209 photoresist. The porous silicon particles were then produced using our proprietary two-step electrochemical etching method in a hydrofluoric acid and ethanol (1:3, v/v) solution as described previously (Godin et al., 2010; Serda et al., 2009c; Tasciotti et al., 2008). The isopropyl alcohol (IPA) particles suspension was transferred to a glass Petri dish and IPA was evaporated using a hotplate set at $60\,°C$ overnight. The hotplate temperature was then raised to $120\,°C$ for 15 min to insure evaporation of residual IPA from the porous matrix. The dried particles were then treated with piranha solution to obtain oxidized negatively charged S1MP and modified with 2% (v/v) 3-aminopropyltriethoxysilane (APTES) (Sigma–Aldrich, St. Louis, MO) for 2 h at room temperature to obtain positively charged S1MP as previously described.

Volumetric particle size, size distribution and count were obtained using a Z2 Coulter® Particle Counter and Size Analyzer (Beckman Coulter, Fullerton, CA, USA). Prior to the analysis, the samples were dispersed in the balanced electrolyte solution (ISOTON® II Diluent, Beckman Coulter Fullerton,

CA, USA) and sonicated for 5 s to ensure a homogenous dispersion.

The zeta potential of the silicon particles was analyzed using a Zetasizer nano ZS (Malvern Instruments Ltd., Southborough, MA, USA). For the analysis, $2\,\mu L$ particle suspension containing at least 2×10^5 particles to give a stable zeta value evaluation were injected into a sample cell countering filed with phosphate buffer (PB, 1.4 mL, pH 7.3). The cell was sonicated for 2 min, and then an electrode-probe was put into the cell. Measurements were conducted at room temperature ($23\,°C$) in triplicates.

2.2. Animals and experimental outline

Male and female FBV mice (5–6 weeks old, 19–24 g, Charles River, USA) were maintained in a VAF-barrier facility in Institute of Molecular Medicine, the University of Texas Health Sciences Center in Houston. All experimental procedures were performed in accordance with the regulation in the University of Texas for the Care and Use of Laboratory Animals. Mice were randomly divided into 14 groups of 4–6 animals and received a single or 4 consecutive weekly injections through the tail vein. In the single administration set-up, the mice were injected with three escalating doses (10^7, 10^8 and 5×10^8 particles in $100\,\mu L$ saline/mice) of negatively charged oxidized particles or positively charged APTES modified S1MP. Control mice received i.v. injections of 0.5 mg of sodium silicate, equivalent to 5×10^8 S1MP and saline alone. For multiple injections study, mice received i.v. injections of S1MP at a dose of 10^8 S1MP per administration once a week for 4 weeks. At the endpoint, the mice were anesthesized and the plasma samples were collected by cardiac puncture and analyzed for blood chemistry and cytokine production. The major organs (liver, spleen, kidney, lung, brain, heart, and thyroid) were harvested, fixed in formalin and processed for histological evaluation (H&E staining). A part of the liver and spleen were snap frozen in liquid nitrogen and stored separately for evaluation of tissue LDH levels.

2.3. Blood chemistry

Hepatic and renal functions were tested to evaluate tissue injury. Lactate dehydrogenase, arginase, urea, and creatinine activity in the plasma were measured using assay kits (BioAssay Systems, Hayward, CA, USA). Tissue homogenate from the liver and spleen were prepared for the measurement of tissue LDH level. The analysis was performed following manufacturer's instructions.

2.4. Cytokines analysis

The sera were isolated from whole blood and stored at $-70\,°C$ until used. Cytokine levels were measured by using a Bio-Plex murine cytokine 23-Plex assay kit (Bio-Rad Laboratories, Hercules, CA) which evaluated the levels of: Eotaxin, IL-1β, IL-1α, IL-2, IL-3, IL-4, IL-5, IL-6, IL-9, IL-10, IL-12 (p40 and p70), IL-13, IL-17, TNF-α, granulocyte colony-stimulating factor (G-CSF), granulocyte/macrophage colony-stimulating factor (GM-CSF), IFN-γ, KC, RANTES, macrophage inflammatory protein (MIP-1α and MIP-1β) and monocyte chemotactic protein-1. The cytokines levels were read on the Luminex 200 System, Multiplex Bio-Assay Analyzer and quantified based on standard curves for each cytokine in the concentration range of 1–32,000 pg/mL.

2.5. Histological examination

The tissues were fixed in formalin and embedded in paraffin. Tissue sections ($5\,\mu m$) were stained with hematoxylin/eosin. Microscopic analysis was performed to evaluate leukocyte infiltration to the tissues. At least five random sections from each slide were examined.

Table 1
Biochemical analysis of plasma samples following single-dose i.v. administration of various S1MP pSi nanovectors. The treatment included saline, silicic acid equivalent to the 5×10^8 of the pSi particles injected, negatively (oxidized) and positively (APTES) charged particles at three doses (10^7, 10^8 and 5×10^8 particles per mouse). The results are presented as mean $\pm$ S.D.

| Treatments	LDH (IU/L)	Arginase (U/L)	Urea (mg/dL)	Creatinine (mg/dL)
Saline	127.0 ± 10.4 ($n=2$)	10.7 ± 2.9 ($n=3$)	55.3 ± 13.8 ($n=4$)	0.43 ± 0.04 ($n=4$)
Silicic acid	82.9 ± 7.2 ($n=4$)	11.6 ± 3.9 ($n=4$)	38.1 ± 3.1 ($n=5$)	0.43 ± 0.01 ($n=4$)
APTES 10^7	99.7 ± 17.4 ($n=5$)	11.1 ± 3.4 ($n=3$)	41.3 ± 4.8 ($n=6$)	0.49 ± 0.03 ($n=5$)
APTES 10^8	115.4 ± 29.1 ($n=5$)	11.9 ± 1.8 ($n=6$)	47.9 ± 9.2 ($n=6$)	0.46 ± 0.08 ($n=6$)
APTES 5×10^8	186.8 ± 22.0 ($n=3$)	9.4 ± 3.0 ($n=5$)	52.1 ± 13.4 ($n=6$)	0.43 ± 0.03 ($n=5$)
Oxidized 10^7	167.2 ± 26.9 ($n=5$)	10.4 ± 3.2 ($n=4$)	58.4 ± 8.6 ($n=6$)	0.48 ± 0.17 ($n=4$)
Oxidized 10^8	145.2 ± 23.6 ($n=4$)	12.8 ± 4.4 ($n=5$)	60.7 ± 6.6 ($n=6$)	0.61 ± 0.09 ($n=3$)
Oxidized 5×10^8	175.7 ± 32.8 ($n=4$)	15.9 ± 2.7 ($n=6$)	49.3 ± 5.5 ($n=6$)	0.5 ± 0.08 ($n=6$)

2.6. Statistical analysis

All experiments were performed at least in quadruplicates. The statistical significance of the data was determined by the Student's *t*-test.

3. Results

To evaluate the biocompatibility of the intravenously injected S1MP (hemispherical shape, Fig. 1), organ functions and immunogenicity were tested in immunocompetent mice in two experimental schedules (acute and subchronic). The zeta potential of the tested S1MP was -32.5 ± 3.1 mV and $+8.7 \pm 2.5$ mV for negatively and positively particles, respectively. In our recent study with multistage delivery system loaded with liposomal siRNA for therapy of ovarian tumors, we used a dose of 10^7 hemispherical S1MP particles/mouse and this system has been shown to be therapeutically efficient with an effect lasting for at least 3 weeks after a single injection (Tanaka et al., 2010). We have chosen this dose as the lowest dose for our tolerability study having also 10 and 50 times higher doses (10^8 and 5×10^8, respectively). For evaluation of hepatic and renal functions, plasma levels of biochemical markers (LDH, arginase, urea, and creatinine) for single (acute) and multiple injections (subchronic) were examined and summarized in Tables 1 and 2, respectively. The S1MP up to 10^8 did not cause an increased release of tissue biomarkers as compared to saline or silicic acid injected mice in acute setting. However, LDH levels were slightly higher in the mice injected with S1MP with both negative and positive charges at the dose of 5×10^8. Similarly, no obvious signs of toxicity in both renal and hepatic functions were noted in the subchronic administration. Histopathological evaluation revealed that S1MPs were accumulated primarily in the liver and spleen with no indication of leukocytes infiltration (Fig. 2). No obvious S1MP accumulation in the kidney, heart, lung, and brain was observed. Because of S1MP accumulation in the liver and spleen, we next tested LDH levels of tissue homogenate from these organs. Intravenous injection of S1MPs did not exhibit significant increase in tissue LDH levels in the liver and spleen as compared to the negative control (saline and silicic acid) at any dose tested in both acute and subchronic setting.

Next, we tested the immunoreactivity of intravenously injected S1MP in both acute and subchronic setting. Fig. 3 summarizes the results of the cytokines levels detected in the acute single-dose
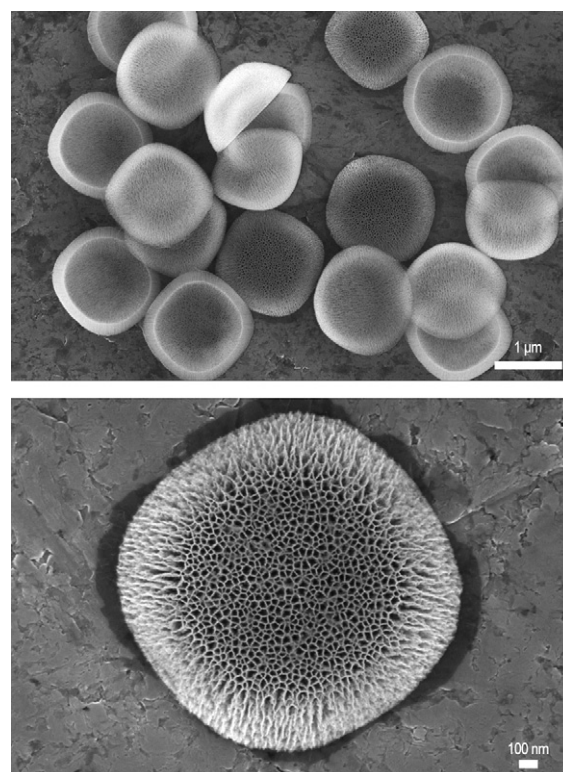

Fig. 1. Scanning Electron Micrographs of hemispherical shaped nanoporous silicon S1MPs used in this study. Low magnification image (5k), showing a uniform size and shape distribution of microfabricated nanocarriers (upper image); and high magnification image (20k) presenting the porous structure of the S1MP where the S2NP can be loaded (lower image).

study. The following cytokines including bEotaxin, GM-CSF, IFN-γ, IL-1β, IL-1α, IL-2, IL-4, IL-5, IL-10, IL-17, MIP-1β and MCP-1, were undetectable in any of the treatment groups injected with different systems and are not included in Figs. 4 and 5. The level of most of the other cytokines was not significantly higher ($p < 0.01$) in any of the tested systems as compared with saline injected control group. The only exception of IL-9 and IL-12, which were slightly elevated in the mice injected with 5×10^8 S1MP. In the multiple dose setting, there were no detectable changes in plasma cytokine levels
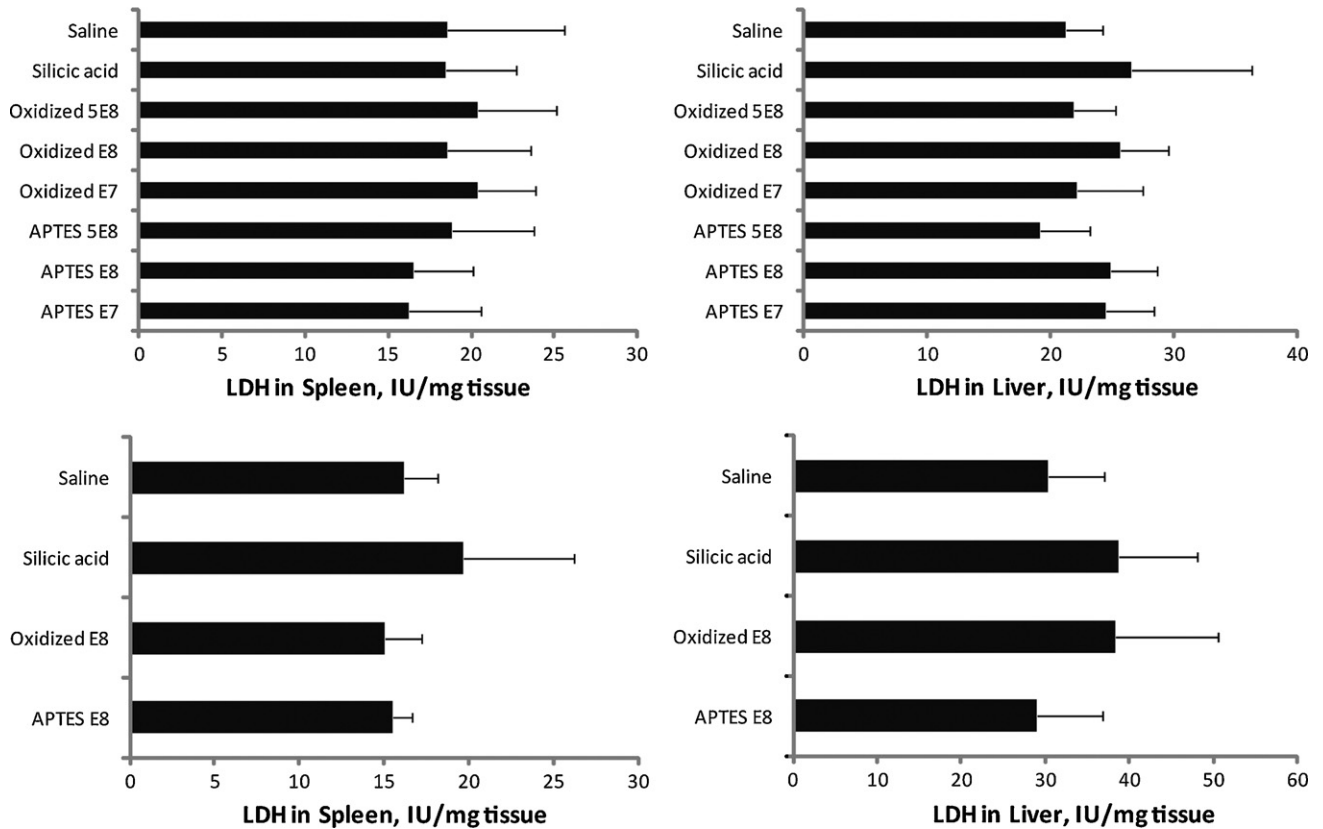
Table 2
Biochemical analysis of plasma samples following multiple dose (four weekly doses) i.v. administration of various S1MPs. The treatments included saline, silicic acid (equivalent to the 10^8 of the S1MP), negatively (oxidized) and positively (APTES) charged particles at the dose of 10^8 particles per mouse. The results are presented as mean $\pm$ S.D.

| Treatments	LDH (IU/L)	Arginase (U/L)	Urea (mg/dL)	Creatinine (mg/dL)
Saline	178.4 ± 74.6 ($n=5$)	18.4 ± 5.31 ($n=5$)	60.1 ± 15.7 ($n=5$)	0.12 ± 0.06 ($n=3$)
Silicic acid	130.8 ± 45.1 ($n=6$)	11.9 ± 9.8 ($n=6$)	57.8 ± 8.7 ($n=7$)	0.06 ± 0.06 ($n=5$)
Oxidized 10^8	155.8 ± 38.4 ($n=6$)	13.6 ± 5.07 ($n=4$)	56.7 ± 6.02 ($n=7$)	0.25 ± 0.19 ($n=7$)
APTES 10^8	135.5 ± 52.3 ($n=6$)	6.0 ± 2.2 ($n=6$)	54.1 ± 5.63 ($n=6$)	0.10 ± 0.06 ($n=6$)
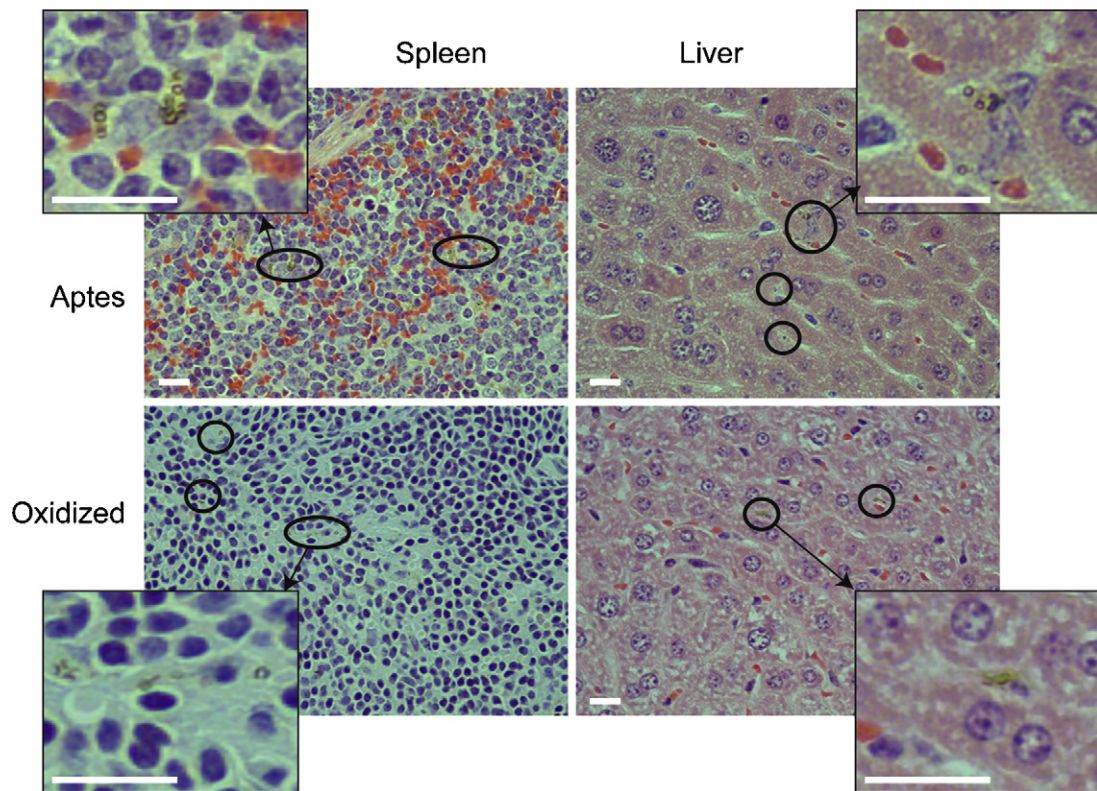
Fig. 2. S1MP tissue accumulation. The liver and spleen were harvested from the mice injected with S1MP (10^8 in saline) via tail vein and fixed with formalin. Five micron paraffin sections were stained with H&E to identify the localization of S1MP. The circles and zoom-in areas indicate the S1MP accumulation in the liver and spleen (final magnification = 400×, bar 20 μm).

Fig. 3. LDH levels in spleen and liver following single (left column) or multiple dose (four weekly doses, right column) i.v. administration of various pSi S1MP nanovectors. Three doses of negatively (oxidized) and positively (APTES) charged pSi particles were injected and saline and silicic acid were used as controls. The results are presented as mean ± S.D.
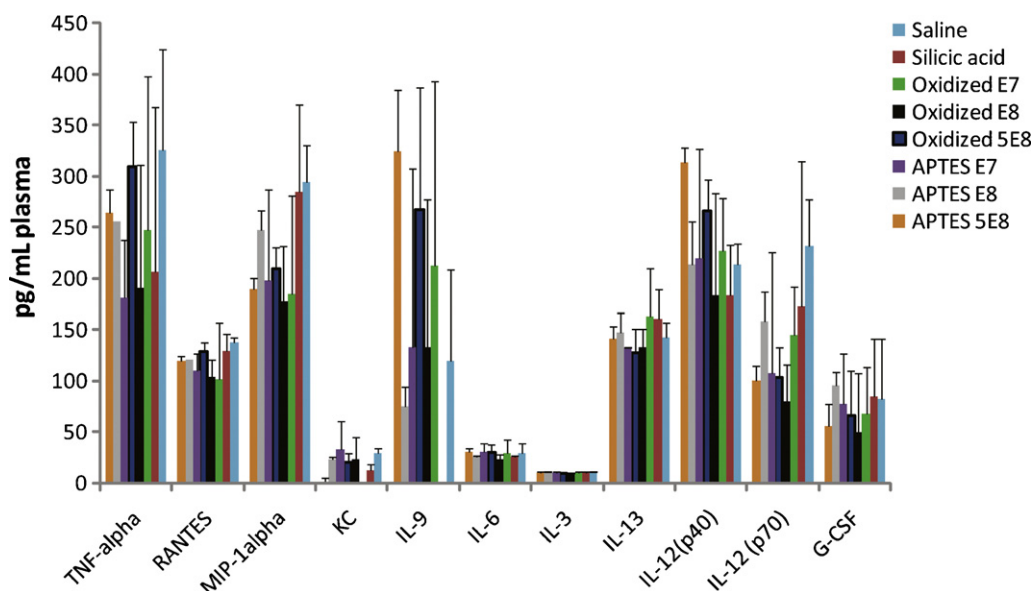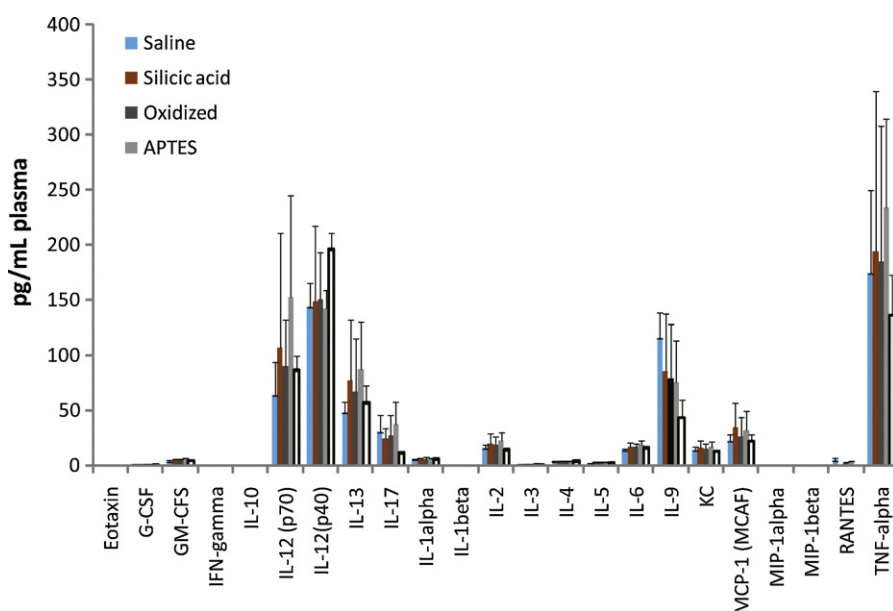
Fig. 4. Plasma cytokine levels 24 h following single dose i.v. administration of various pSi S1MP nanovectors. The treatments included saline, silicic acid equivalent to the 5×10^8 of the particles injected, negatively (oxidized) and positively (APTES) charged S1MP particles at the doses of 10^7, 10^8 and 5×10^8 particles per mouse. The results are presented as mean $\pm$ S.D. ($n = 4$–6).

of S1MP injected mice as compared to the control group. Interestingly, in the long-term study slightly lower levels of cytokines were generally detected (also for saline injected mice). This difference may be attributed to the manipulation (e.g. intravenous injection) itself since the end point of each experiment was placed differently (24 h after the acute setting vs. 7 days after the last injection in the subchronic setting).

Clinical observation of the mice in both acute and subchronic administration regimens did not reveal any cases of mortality in the treated and control groups. There were no signs of abnormal behavioral reactions and general clinical symptoms. No statistically significant differences in the body weight gain were observed between various treatment groups and control mice in subchronic setting.

4. Discussion

On the basis of degradability of pSi under the physiological conditions, pSi is highlighted as one of the emerging biomaterials and is currently being intensively investigated for various clinical applications. Unlike bulk silicon, porous silicon is biocompatible and current clinically used silicon-based biomedical application include BioSilicon[TM] (pSivida Corp.) for drug delivery, and two FDA-approved sustained release devices for the treatment of chronic eye disease (www.psivida.com). We proposed a multi-stage vector (MSV) system that is comprised of biodegradable porous silicon particles loaded with nanoparticles (Tasciotti et al., 2008). The concept behind this carrier is decoupling various functionalities and combining multiple delivery vectors in one construct which will

Fig. 5. Plasma cytokine levels following multiple dose (four weekly doses) i.v. administration of various pSi S1MP nanovectors. The animals were sacrificed on the 5th week from the first injection. The treatments included saline, silicic acid equivalent to the 10^8 of the S1MP particles injected, negatively (oxidized) and positively (APTES) charged particles at the dose of 10^8 particles per mouse ($n = 4$–6).

enable their synergistic and sequential action with the main application in oncology. Our very recent study has shown that MSV efficiently deliver siRNA to ovarian tumors in a sustained mode, and require several times less frequent dosing regimens than siRNA liposomes bearing the same dose of the therapeutic (Tanaka et al., 2010).

Oxidation of the silicon surface generates hydroxyl units imparting the negative zeta potential to the S1MP, while conjugation of APTES molecules inverts the zeta potential to the positive. Both states can be used for subsequent functionalization of pSi with ligand for active targeting or PEGylation (Godin et al., 2010). Silicon is an essential trace element in the body, deposited into connective tissue, cartilage and bone (Carlisle, 1970). However, some forms of crystalline silicon dioxide are known to be cytotoxic to macrophages (Absher et al., 1989; Kolb-Bachofen, 1992; Wilson et al., 1981). Thus, it is important to assess safety of the S1MP with two different surface modifications (positive and negative charge). The reports on biocompatibility of porous silicon (pSi) launched in 1995 by Canham's group, which have shown that unlike bulk silicon, pSi degrades with regards to porosity and pore size (Canham, 1995). The main degradation product of pSi is silicic acid ($Si(OH)_4$), the most abundant form of the Si in the environment. In the Western world the average daily dietary intake of silicon, the essential body mineral, is 20–50 mg (Jugdaohsingh et al., 2002). Highly porous Si (porosity >50%) dissolves in the majority of the simulated biological fluids including serum and PBS, except for the acidic environment such as the simulated gastric fluid (Anglin et al., 2008). Later it was shown that, the biodegradation of pSi structures was shown to be dependent on the porosity and the surface modifications (Godin et al., 2010). Since then numerous reports have been published dealing with in vitro interactions of pSi structures with biological substances such as biodegradation in physiological conditions (Godin et al., 2010), calcification (Whitehead et al., 2008), cell adhesion (Alvarez et al., 2009), interaction with neuron interfaces neural networks (Moxon et al., 2007) and protein adsorption (Hu et al., 2007). To date, however, a limited number of in vivo assessments of tissue compatibility of porous silicon have been carried out (Low et al., 2009) and to the best of our knowledge none of these studies has dealt with systemically injectable pSi.

Various delivery carriers derived from different materials are being developed. Nevertheless, despite superiority in delivery efficacy, medical applications of many of the delivery carriers are limited due to a lack of biocompatibility. Therefore, it is essential to develop biocompatible delivery carriers for successful and safe medical applications. Currently, there are no specific guidelines on how the safety of nanostructured materials should be tested and these are being unified (Dobrovolskaia et al., 2008, 2009; Hall et al., 2007). Particulates, in general, have been long known to be a possible source of local irritation initiating an inflammatory response due to their physical, chemical or biological properties (e.g. asbestos), which can be either acute or chronic. Acute inflammation quickly resolves in healing, while chronic inflammation is a continuing condition characterized by a polymorphonuclear leucocyte infiltration of tissue. Type of material, physico-chemical properties, and geometry of delivery carriers are crucial parameters and collectively contribute to biocompatibility. In the last decade, a number of papers have described the toxicology of newly engineered nanomaterials, including fullerenes (Sayes et al., 2005), carbon nanotubes (Donaldson et al., 2006), quantum dots (Hardman, 2006). These reports have demonstrated that a variety of factors can affect evaluation of toxic responses from nanomaterials and that only limited toxicity data is currently available. In the present study we investigated the biocompatibility of the microfabricated S1MPs following a single and multiple dose administration in immunocompetent mice. We examined three parameters for safe systemic application of porous silicon particles; cytotoxicity,

immunoreactivity and altered histology of major organs. It is possible that a sampling point at 24 h following injection can mask some transient acute reactions. This time-point was chosen based on the in vitro studies with immune and endothelial cells in which the reaction to positive control (zymosan) picked at 24 h (Godin et al., 2010; Serda et al., 2009b). There is a negligible concentration of the hemispherical particles in circulation 6 h following the administration, however, since the majority of the particles are still in the body after 24 h, as it was shown in the study by Tanaka et al. (2010), we do not anticipate that the acute response will be diminished at this time frame. For drug delivery application, one of the most prominent determinants of the cytotoxicity of injectable foreign materials is the evaluation of hepatic and renal functions. Slight elevation in plasma LDH levels was observed with the highest dose of the S1MPs (5×10^8) injected mice in the acute setting. Some of the organs relatively rich in LDH are the heart, kidney, liver, spleen and muscle. Histological slides of these organs were examined and no pathological findings were detected. Elevated plasma LDH levels can also be an indication of injury (e.g. tail vein injection). Based on our previous studies, the main organs were the S1MP carrier is concentrated are liver and spleen. LDH activity was not increased in these organs. No increase in the tested biochemical parameters was observed in plasma or tissue levels also in subchronic setting, suggesting that the hemispherical shape S1MPs with 1.6 μm diameter with 50% porosity are well tolerated both in single and sub-chronic multiple administrations.

Macrophage recognition and ingestion of foreign particles is of considerable importance for the maintenance of tissue homeostasis and in resolution of inflammation. Macrophages provide the first line of defense against microorganisms and other foreign materials including particles. It is known that cellular uptake of the engineered nanomaterials can be modulated through the surface modifications, size and shape of the particles (Champion and Mitragotri, 2006; Evora et al., 1998; Serda et al., 2009d). For example, it was shown that monodisperse silica nanoparticles affect endothelial cells in a size-dependent manner: the larger are the particles – the cytotoxic effects are less pronounced (Nabeshi et al., 2010; Napierska et al., 2009). Similarly, in a study with polystyrene particles there was a significantly greater neutrophil influx into the rat lung, accompanied with increased cytokine, protein and LDH levels in broncheoalveolar lavage after instillation of 64-nm particles as compared to 202 and 535-nm particles (Brown et al., 2001). Multistage carrier is comprised of relatively large biodegradable non-spherical particles, S1MP, which marginate and adhere more efficiently to the tumor vasculature (Ferrari, 2010). These particles are further loaded with smaller nanocarriers (Tasciotti et al., 2008) which are released at the right time and place, avoiding various barriers en route to the disease site. Precisely microfibricated S1MP are >400 nm in diameter (Chiappini et al., 2010) which allows them to accommodate smaller nanoparticles in the porous structure. This feature can explain the lack of toxicity of S1MP as compared to smaller silica particles. Though there is still sparse information on the mode of uptake of engineered nanomaterials by macrophages, their major response to stimuli is the release of cytokines, which can promote the cascade of inflammatory response to foreign substances (Cerami, 1992; Kenneth Ward, 2008). Increased levels of cytokines in plasma following intravenous injections of two types of S1MP with the highest doses were assessed. In general, rigidity and positive surface charge of foreign material facilitate macrophage uptake, and as expected, both S1MP particles with positive and negative charge were phagocytosed by blood monocytes as well as tissue macrophages. However, uptake of the 1.6 μm in diameter, hemispherical S1MP by macrophages did not induce pre-inflammatory (IL-6 and TNF-α) cytokine production and did not affect the levels of Th1- and Th2-associated cytokines (i.e. IL-1, IL-2, IL-4, IL-6, IL-10 and IFN-γ). Liu et al. reported that

fullerene derivatives $C_{60}(OH)_{20}$ increased the production of such proinflammatory cytokines TNF-α, INF-β and IL-2 by more 10–20 times (Liu et al., 2009). We observed a slight increase (2–3 times) in the plasma levels of IL-9 after the injection of the highest does of S1MP (5×10^8). IL-9 belongs to the Th2 cytokine family, has recently been implicated as an essential factor in determining mucosal immunity and susceptibility to atopic asthma. Plasma levels of the other Th2 related cytokines such as IL-4, IL-5 and IL-13 were not increased. Our in vivo results are in line with the previous in vitro data on response of endothelial cells (HUVEC; human) and macrophages to S1MPs. While positive control zymosan particles elicited a prominent increase in cytokine production, we did not find a significant increase following S1MP exposure for 1, 4, and 24 h. Preservation of cellular morphology, cell viability, impact on cell cycle, mitotic potential and pro-inflammatory responses following cellular engulfment of S1MPs have also been demonstrated (Godin et al., 2010; Serda et al., 2009b). Moreover, endothelial cells with internalized S1MP undergo normal cellular proliferation, and cells with as many as 30 internalized S1MP display even partitioning of particle-bearing endosomes to daughter cells during mitosis. In our present study, we did not find significant inflammatory responses (both innate and adaptive immunity) following either acute or sub-chronic administration. In a study by Witasp et al. mesoporous of different sizes silica particles with cubic pore geometries were shown to be efficiently internalized by primary human monocyte-derived macrophages. Uptake of pSi particles was independent of serum factors and did not impair cell viability or function of macrophages, including the ingestion of different classes of apoptotic or opsonized target cells (Witasp et al., 2009).

Multistage delivery system is a platform technology for encapsulation of a variety of S2NP into a rationally designed porous silicon nanocarrier, S1MP, aiming at overcoming sequential biophysical barriers in tumors (Tasciotti et al., 2008). Thus, it was important to first check the in vivo biocompatibility of S1MP. Any type of S2NP may have an effect on the overall safety profile of the system. Data from recently published studies with siRNA liposomes loaded S1MP and iron oxide S2NP demonstrate that no toxic effect were observed in vivo and in vitro (Godin et al., 2010; Serda et al., 2009b; Tanaka et al., 2010). Currently ongoing studies are focused on other therapeutic/diagnostic MSV systems for applications in oncology.

In conclusion, we demonstrate that acute or subchronic intravenous administration of the porous silicon micro particles (S1MP) did not produce obvious changes in blood chemistry and immunoreactivity in mice.

Acknowledgements

References

Absher, M.P., Trombley, L., Hemenway, D.R., Mickey, R.M., Leslie, K.O., 1989. Biphasic cellular and tissue response of rat lungs after eight-day aerosol exposure to the silicon dioxide cristobalite. Am. J. Pathol. 134, 1243–1251.

Alvarez, S.D., Derfus, A.M., Schwartz, M.P., Bhatia, S.N., Sailor, M.J., 2009. The compatibility of hepatocytes with chemically modified porous silicon with reference to in vitro biosensors. Biomaterials 30, 26–34.

Anglin, E.J., Cheng, L., Freeman, W.R., Sailor, M.J., 2008. Porous silicon in drug delivery devices and materials. Adv. Drug Deliv. Rev. 60, 1266–1277.

Brown, D.M., Wilson, M.R., MacNee, W., Stone, V., Donaldson, K., 2001. Size-dependent proinflammatory effects of ultrafine polystyrene particles: a role for surface area and oxidative stress in the enhanced activity of ultrafines. Toxicol. Appl. Pharmacol. 175, 191–199.

Canham, L.T., 1995. Bioactive silicon structure fabrication through nanoetching techniques. Adv. Mater. 7, 1033–1037.

Canham, L.T., 1999. Properties of porous silicon. Crystal Research and Technology, vol. 34. Wiley-VCH.

Carlisle, E.M., 1970. Silicon: a possible factor in bone calcification. Science 167, 279–280.

Cerami, A., 1992. Inflammatory cytokines. Clin. Immunol. Immunopathol. 62, S3–10.

Champion, J.A., Mitragotri, S., 2006. Role of target geometry in phagocytosis. Proc. Natl. Acad. Sci. U.S.A. 103, 4930–4934.

Chiappini, C., Tasciotti, E., Fakhoury, J.R., Fine, D., Pullan, L., Wang, Y.C., Fu, L., Liu, X., Ferrari, M., 2010. Tailored porous silicon microparticles: fabrication and properties. Chemphyschem 11, 1029–1035.

Cohen, M.H., Melnik, K., Boiarski, A.A., Ferrari, M., Martin, F.J., 2003. Microfabrication of silicon-based nanoporous particulates for medical applications. Biomed. Microdevices 5, 253–259.

Decuzzi, P., Lee, S., Ferrari, M., 2004. Adhesion of microfabricated particles on vascular endothelium: a parametric analysis. Ann. Biomed. Eng. 32, 793–802.

Dobrovolskaia, M.A., Aggarwal, P., Hall, J.B., McNeil, S.E., 2008. Preclinical studies to understand nanoparticle interaction with the immune system and its potential effects on nanoparticle biodistribution. Mol. Pharm. 5, 487–495.

Dobrovolskaia, M.A., Germolec, D.R., Weaver, J.L., 2009. Evaluation of nanoparticle immunotoxicity. Nat. Nanotechnol. 4, 411–414.

Donaldson, K., Aitken, R., Tran, L., Stone, V., Duffin, R., Forrest, G., Alexander, A., 2006. Carbon nanotubes: a review of their properties in relation to pulmonary toxicology and workplace safety. Toxicol. Sci. 92, 5–22.

Evora, C., Soriano, I., Rogers, R.A., Shakesheff, K.N., Hanes, J., Langer, R., 1998. Relating the phagocytosis of microparticles by alveolar macrophages to surface chemistry: the effect of 1,2-dipalmitoylphosphatidylcholine. J. Control. Release 51, 143–152.

Ferrari, M., 2010. Frontiers in cancer nanomedicine: transport oncophysics and logic-embedded vectors. Trends Biotechnol. 28 (4), 181–188.

Godin, B., Gu, J., Serda, R.E., Bhavane, R., Tasciotti, E., Chiappini, C., Liu, X., Tanaka, T., Decuzzi, P., Ferrari, M., 2010. Tailoring the degradation kinetics of mesoporous silicon structures through PEGylation. J. Biomed. Mater. Res. A 94 (4), 1236–1243.

Hall, J.B., Dobrovolskaia, M.A., Patri, A.K., McNeil, S.E., 2007. Characterization of nanoparticles for therapeutics. Nanomedicine (London) 2, 789–803.

Hardman, R., 2006. A toxicologic review of quantum dots: toxicity depends on physicochemical and environmental factors. Environ. Health Perspect. 114, 165–172.

Hu, L., Xu, S., Pan, C., Zou, H., Jiang, G., 2007. Preparation of a biochip on porous silicon and application for label-free detection of small molecule-protein interactions. Rapid Commun. Mass Spectrom. 21, 1277–1281.

Jugdaohsingh, R., Anderson, S.H., Tucker, K.L., Elliott, H., Kiel, D.P., Thompson, R.P., Powell, J.J., 2002. Dietary silicon intake and absorption. Am. J. Clin. Nutr. 75, 887–893.

Kenneth Ward, W., 2008. A review of the foreign-body response to subcutaneously-implanted devices: the role of macrophages and cytokines in biofouling and fibrosis. J. Diabetes Sci. Technol. 2, 768–777.

Kolb-Bachofen, V., 1992. Uptake of toxic silica particles by isolated rat liver macrophages (Kupffer cells) is receptor mediated and can be blocked by competition. J. Clin. Invest. 90, 1819–1824.

Lee, S.Y., Ferrari, M., Decuzzi, P., 2009. Shaping nano-/micro-particles for enhanced vascular interaction in laminar flows. Nanotechnology 20, 495101.

Lehmann, V., Gosele, U., 1991. Porous silicon formation: a quantum wire effect. Appl. Phys. Lett. 58, 656–658.

Li, Y.Y., Cunin, F., Link, J.R., Gao, T., Betts, R.E., Reiver, S.H., Chin, V., Bhatia, S.N., Sailor, M.J., 2003. Polymer replicas of photonic porous silicon for sensing and drug delivery applications. Science 299, 2045–2047.

Lin, V.S., Motesharei, K., Dancil, K.P., Sailor, M.J., Ghadiri, M.R., 1997. A porous silicon-based optical interferometric biosensor. Science 278, 840–843.

Liu, Y., Jiao, F., Qiu, Y., Li, W., Qu, Y., Tian, C., Li, Y., Bai, R., Lao, F., Zhao, Y., et al., 2009. Immunostimulatory properties and enhanced TNF-alpha mediated cellular immunity for tumor therapy by $C_{60}(OH)_{20}$ nanoparticles. Nanotechnology 20, 415102.

Low, S.P., Voelcker, N.H., Canham, L.T., Williams, K.A., 2009. The biocompatibility of porous silicon in tissues of the eye. Biomaterials 30, 2873–2880.

Martin, K.R., 2007. The chemistry of silica and its potential health benefits. J. Nutr. Health Aging 11, 94–97.

Moxon, K.A., Hallman, S., Aslani, A., Kalkhoran, N.M., Lelkes, P.I., 2007. Bioactive properties of nanostructured porous silicon for enhancing electrode to neuron interfaces. J. Biomater. Sci. Polym. Ed. 18, 1263–1281.

Nabeshi, H., Yoshikawa, T., Matsuyama, K., Nakazato, Y., Arimori, A., Isobe, M., Tochigi, S., Kondoh, S., Hirai, T., Akase, T., et al., 2010. Size-dependent cytotoxic effects of amorphous silica nanoparticles on Langerhans cells. Pharmazie 65, 199–201.

Napierska, D., Thomassen, L.C., Rabolli, V., Lison, D., Gonzalez, L., Kirsch-Volders, M., Martens, J.A., Hoet, P.H., 2009. Size-dependent cytotoxicity of monodisperse silica nanoparticles in human endothelial cells. Small 5, 846–853.

Nijdam, A.J., Ming-Cheng Cheng, M., Geho, D.H., Fedele, R., Herrmann, P., Killian, K., Espina, V., Petricoin 3, E.F., Liotta, L.A., Ferrari, M., 2007. Physicochemically modified silicon as a substrate for protein microarrays. Biomaterials 28, 550–558.

Nijdam, A.J., Zianni, M.R., Herderick, E.E., Cheng, M.M., Prosperi, J.R., Robertson, F.A., Petricoin, E.F., Liotta, L.A., Ferrari, M., 2009. Application of physicochemically

modified silicon substrates as reverse-phase protein microarrays. J. Proteome Res. 8, 1247–1254.

Riehemann, K., Schneider, S.W., Luger, T.A., Godin, B., Ferrari, M., Fuchs, H., 2009. Nanomedicine—challenge and perspectives. Angew Chem. Int. Ed. Engl. 48, 872–897.

Ruoslahti, E., 2004. Vascular zip codes in angiogenesis and metastasis. Biochem. Soc. Trans. 32, 397–402.

Sakamoto, J., Annapragada, A., Decuzzi, P., Ferrari, M., 2007. Antibiological barrier nanovector technology for cancer applications. Expert Opin. Drug Deliv. 4, 359–369.

Salonen, J., Kaukonen, A.M., Hirvonen, J., Lehto, V.P., 2008. Mesoporous silicon in drug delivery applications. J. Pharm. Sci. 97, 632–653.

Salonen, J., Laitinen, L., Kaukonen, A.M., Tuura, J., Bjorkqvist, M., Heikkila, T., Vaha-Heikkila, K., Hirvonen, J., Lehto, V.P., 2005. Mesoporous silicon microparticles for oral drug delivery: loading and release of five model drugs. J. Control. Release 108, 362–374.

Sayes, C.M., Gobin, A.M., Ausman, K.D., Mendez, J., West, J.L., Colvin, V.L., 2005. Nano-C60 cytotoxicity is due to lipid peroxidation. Biomaterials 26, 7587–7595.

Serda, R.E., Chiappini, C., Fine, D., Tasciotti, E., Ferrari, M., 2009a. Porous silicon particles for imaging and therapy of cancer. In: Kumar, C.S.S.R. (Ed.), Nanomaterials for the Life Sciences. Wiley-VCH, p. 359.

Serda, R.E., Ferrati, S., Godin, B., Tasciotti, E., Liu, X., Ferrari, M., 2009b. Mitotic partitioning of silicon microparticles. Nanoscale 1, 250–259.

Serda, R.E., Gu, J., Bhavane, R.C., Liu, X., Chiappini, C., Decuzzi, P., Ferrari, M., 2009c. The association of silicon microparticles with endothelial cells in drug delivery to the vasculature. Biomaterials 30, 2440–2448.

Serda, R.E., Gu, J., Burks, J.K., Ferrari, K., Ferrari, C., Ferrari, M., 2009d. Quantitative mechanics of endothelial phagocytosis of silicon microparticles. Cytometry A 75, 752–760.

Sharma, S., Nijdam, A.J., Sinha, P.M., Walczak, R.J., Liu, X., Cheng, M.M., Ferrari, M., 2006. Controlled-release microchips. Expert Opin. Drug Deliv. 3, 379–394.

Tanaka, T., Mangala, L.S., Vivas-Mejia, P.E., Nieves-Alicea, R., Mann, A.P., Mora, E., Han, H.-D., Shahzad, M.M.K., Liu, X., Bhavane, R., et al., 2010. Sustained siRNA delivery by mesoporous silicon particles. Cancer Res..

Tasciotti, E., Liu, X., Bhavane, R., Plant, K., Leonard, A.D., Price, B.K., Cheng, M.M., Decuzzi, P., Tour, J.M., Robertson, F., Ferrari, M., 2008. Mesoporous silicon particles as a multistage delivery system for imaging and therapeutic applications. Nat. Nanotechnol. 3, 151–157.

Whitehead, M.A., Fan, D., Mukherjee, P., Akkaraju, G.R., Canham, L.T., Coffer, J.L., 2008. High-porosity poly(epsilon-caprolactone)/mesoporous silicon scaffolds: calcium phosphate deposition and biological response to bone precursor cells. Tissue Eng. Part A 14, 195–206.

Wilson, J., Pigott, G.H., Schoen, F.J., Hench, L.L., 1981. Toxicology and biocompatibility of bioglasses. J. Biomed. Mater. Res. 15, 805–817.

Witasp, E., Kupferschmidt, N., Bengtsson, L., Hultenby, K., Smedman, C., Paulie, S., Garcia-Bennett, A.E., Fadeel, B., 2009. Efficient internalization of mesoporous silica particles of different sizes by primary human macrophages without impairment of macrophage clearance of apoptotic or antibody-opsonized target cells. Toxicol. Appl. Pharmacol. 239, 306–319.